Journal of Systems Engineering and Electronics
Vol. 33, No. 3, June 2022, pp.706 – 715

Exact uncertainty compensation of linear systems by continuous fixed-time output-feedback controller

SHI Shang[1,2], ZHANG Guosheng[1], MIN Huifang[3,*], HU Yinlong[1], and SUN Yonghui[1]

1. College of Energy and Electrical Engineering, Hohai University, Nanjing 211100, China; 2. School of Automation, Southeast University, Nanjing 234299, China; 3. School of Automation, Nanjing University of Science and Technology, Nanjing 210094, China

Abstract: This paper studies the fixed-time output-feedback control for a class of linear systems subject to matched uncertainties. To estimate the uncertainties and system states, we design a composite observer which consists of a high-order sliding mode observer and a Luenberger observer. Then, a robust output-feedback controller with fixed-time convergence guarantee is constructed. Rigorous theoretical proof shows that with the proposed controller, the system states can converge to zero in fixed-time free of the initial conditions. Finally, simulation comparison with existing algorithms is given. Simulation results verify the effectiveness of the proposed controller in terms of its fixed-time convergence and perfect disturbance rejection.

Keywords: linear system, output feedback, matched uncertainty, fixed-time control, observer.

DOI: 10.23919/JSEE.2022.000065

1. Introduction

Uncertainties always exist in practical systems owing to the existence of disturbances, unknown parameters, unmodelled dynamics, etc [1−4]. Hence, the control of systems with uncertainties has attracted much attention in recent years. Discontinuous control techniques such as sliding mode control (SMC) have been widely used to handle bounded and matched uncertainties [5]. However, these algorithms suffer from serious chattering. Although the chattering problem can be reduced to some extent by high-order SMC, it still exists for the discontinuous control input [6−8]. Moreover, in many practical systems, it is difficult to measure all the state signals [9,10]. If only partial state signals are available, one need to design output-feedback controller which is not an easy work.

Manuscript received December 12, 2020.
*Corresponding author.
This work was supported by the National Natural Science Foundation of China (62003131; 62073121; 62173125) and the Natural Science Foundation of Jiangsu Province (BK20200520) .

Finite-time exact observer has been widely used to solve the above problem [11,12]. Output-feedback controllers can be constructed by estimating the system uncertainties and states with the finite-time observer and compensating system uncertainties with the estimated values. In [13], to improve the observation accuracy, a hierarchical high-order sliding mode observer (HOSMO) was developed by modifying the hierarchical super-twisting observer proposed in [11]. Then, based on the proposed hierarchical HOSMO, an output-feedback controller was finally designed. It is noted that the output-feedback [14,15], by combining the HOSMO with finite-time control, continuous finite-time output-feedback controllers were designed to achieve finite-time output regulation.

Note that the conventional asymptotic control has infinite convergence time. In the past decades, finite-time control has been widely investigated for its better precision and faster convergence speed than the asymptotic control. However, the convergence time of the finite-time control as well as the asymptotic control is dependent of the system initial conditions [16,17]. In [18,19] the fixed-time stability concept was proposed to overcome this drawback. While retaining the advantages of finite time control, fixed-time control also has the advantage that the settling time does not depend on the system initial conditions. For the remarkable advantages of fixed-time control, many interesting results have been reported recently [20−23]. In [24], a novel fixed-time continuous controller was designed for an arbitrary dimension integrators by full-state feedback. Later, a continuous fixed-time output feedback controller was proposed in [25] for second-order integrators. It can be clearly observed that the algorithms in [24,25] are only designed for systems without considering any uncertainties. To handle matched system uncertainties, some results about fixed-time SMC have been developed recently [26–28]. However, as has been mentioned previously that these algorithms suffer from serious chattering, which will prevents their application. Furthermore, all these algorithms in [26–28] are designed by full-state feedback. Hence, how to design a robust controller by using fixed-time output-feedback for uncertain systems is the main motivation of this paper.

In this paper, the above problem will be solved. The contributions are mainly two folds: (i) The first fold is that a new composite fixed-time observer consisting of a HOSMO and a Luenberger observer (LO) is presented. Compared with the existing finite-time observer [11–15] whose settling time is dependent on the initial error conditions, our proposed composite observer can achieve fixed-time observation with settling time independent of the initial error conditions. When compared with the existing fixed-time observer [29–31], the fixed-time exact observation of the system states as well as the system uncertainties is achieved for the first time. (ii) By using an exact uncertainty compensation method, a robust output-feedback controller with fixed-time convergence guarantee is constructed. Compared with [26–28] where the full-state information is required and the chattering problem exists, the proposed continuous controller has no chattering problem. Moreover, with the proposed controller, the system states can converge to zero in a fixed-time free of the system initial conditions.

The structure of the paper is as follows: The problem statement is given in the Section 2. Controller design is presented in Section 3. The last two sections are the simulation and conclusion, respectively. In the rest of the paper, we denote $\lfloor x \rceil^{\alpha} = |x|^{\alpha}\text{sign}(x)$ for $\forall \alpha > 0, x \in \mathbf{R}$. The vector norm and matrix norm are chosen as $\|\boldsymbol{x}\| = \sqrt{\boldsymbol{x}^{\mathrm{T}}\boldsymbol{x}}$ ($\boldsymbol{x} \in \mathbf{R}^n$) and $\|\boldsymbol{X}\| = \sqrt{\lambda_{\max}(\boldsymbol{X}^{\mathrm{T}}\boldsymbol{X})}$ ($\boldsymbol{X} \in \mathbf{R}^{n\times n}$), where $\lambda_{\max}(\cdot)$ denotes the maximum eigenvalue of a square matrix. $\boldsymbol{x}^{\mathrm{T}}$ and $\boldsymbol{X}^{\mathrm{T}}$ are the transposes of vector $\boldsymbol{x}$ and matrix $\boldsymbol{X}$, respectively. $\boldsymbol{X}^{-1}$ is used to denote the inverse of matrix $\boldsymbol{X}$.

2. Problem formulation

The system considered here is described as

$$\begin{cases} \dot{\boldsymbol{x}}(t) = \boldsymbol{A}\boldsymbol{x}(t) + \boldsymbol{B}u(t) + \boldsymbol{\psi}(t,\boldsymbol{x}) \\ y(t) = \boldsymbol{C}\boldsymbol{x}(t) \end{cases} \tag{1}$$

where $u(t) \in \mathbf{R}$ and $y(t) \in \mathbf{R}$ is the control input and system output, respectively; $\boldsymbol{x}(t) = [x_1(t), x_2(t), \cdots, x_n(t)]^{\mathrm{T}} \in \mathbf{R}^n$ is the system state; $\boldsymbol{A} \in \mathbf{R}^{n\times n}, \boldsymbol{B} \in \mathbf{R}^{n\times 1}$ and $\boldsymbol{C} \in \mathbf{R}^{1\times n}$ are known matrices; $\boldsymbol{\psi}(t,\boldsymbol{x}) : \mathbf{R}_+ \times \mathbf{R}^n \to \mathbf{R}^n$ is unknown function.

Assumption 1 $\boldsymbol{\psi}(t,\boldsymbol{x})$ satisfies the matched condition, i.e., there exists a known constant $\varphi_{\max}$ such that $\boldsymbol{\psi}(t,\boldsymbol{x}) = \boldsymbol{B}\varphi(t,\boldsymbol{x})$ with $|\dot{\varphi}(t,\boldsymbol{x})| \leqslant \varphi_{\max}$. Moreover, the pair $(\boldsymbol{A},\boldsymbol{B})$ is controllable.

Assumption 2 (Strongly observable of system (1)) For system (1), the relative degree of y with respect to $\varphi(t,\boldsymbol{x})$ is n.

Remark 1 For the control of uncertain linear systems, the matched condition in Assumption 1 is very common. Assumption 2 is also a necessary assumption for finite-time exact observation of the systems with unknown inputs (see, e.g., [11,12]).

The objective of this paper is to construct a robust controller for system (1) by output-feedback such that the system state can be driven to zero in a fixed-time independent of system initial conditions.

2.1 Global finite-time and fixed-time stability

To achieve the control goal, some definitions about the finite-time and fixed-time stability are introduced firstly.

Definition 1[32] Consider the following system:

$$\begin{cases} \dot{\boldsymbol{x}} = \boldsymbol{f}(t,\boldsymbol{x}) \\ \boldsymbol{x}(0) = \boldsymbol{x}_0 \end{cases} \tag{2}$$

where $\boldsymbol{x} \in \mathbf{R}^n$ and $\boldsymbol{f} : \mathbf{R}_+ \times \mathbf{R}^n \to \mathbf{R}^n$ is a nonlinear function that can be discontinuoused. The solutions of system (2) are understood in the Filippov sense [33]. If there exists a time $T(\boldsymbol{x}_0)$, where $T : \mathbf{R}^n \to \mathbf{R}_{\geqslant 0}$ is the settling-time function, such that any solution of system (2) satisfies $\boldsymbol{x}(t,\boldsymbol{x}_0) \equiv \mathbf{0}$ for $\forall t \geqslant T(\boldsymbol{x}_0)$, then we say that the origin of system (2) is globally finite-time stable (GFTS).

Definition 2[34] If there exists a time $T_{\max}$ independent of the system initial values and $\delta > 0$ such that any solution of the system (2) satisfies $\|\boldsymbol{x}(t,\boldsymbol{x}_0)\| \leqslant \delta$ for $\forall t \geqslant T_{\max}$, we say that system (2) is globally practically fixed-time stable (GPFxTS). If $\delta = 0$, then we say that the origin of system (2) is globally fixed-time stable (GFxTS).

2.2 Homogeneity

The following definition of homogeneity is also introduced.

Definition 3 For any $r_i > 0 (i = 1,2,\cdots,n)$ and $\lambda > 0$, define the dilation matrix $\boldsymbol{\Lambda}_r(\lambda) = \text{diag}(\lambda^{r_1}, \lambda^{r_2}, \cdots, \lambda^{r_n})$ and the vector of weights $\boldsymbol{r} = [r_1, r_2, \cdots, r_n]^{\mathrm{T}}$.

(i) For a function $g : \mathbf{R}^n \to \mathbf{R}$, if there exists $d \in \mathbf{R}$ such that for any $\boldsymbol{x} \in \mathbf{R}^n$, the relation $g(\boldsymbol{\Lambda}_r(\lambda)\boldsymbol{x}) = \lambda^d g(\boldsymbol{x})$ holds, then the function g is called r-homogeneous with homogeneity degree d.

(ii) For a vector $\boldsymbol{f} : \mathbf{R}^n \to \mathbf{R}^n$, if there exists $d \geqslant -\min\{r_1, r_2, \cdots, r_n\}$ such that for any $\boldsymbol{x} \in \mathbf{R}^n$, the relation $\boldsymbol{f}(\boldsymbol{\Lambda}_r(\lambda)\boldsymbol{x}) = \lambda^d \boldsymbol{\Lambda}_r(\lambda)\boldsymbol{f}(\boldsymbol{x})$ holds, then the vector $\boldsymbol{f}$ is called r-homogeneous with homogeneity degree d.

3. Robust fixed-time output feedback control

In this section, to estimate the system uncertainty and state, a composite observer consisting of a HOSMO and a LO is constructed. Then, based on the proposed fixed-time observer, a continuous fixed-time output-feedback controller is developed. Finally, the main result is summarized.

3.1 Observer design

The composite observer is designed as follows:

(i) LO design

Firstly, we construct the following LO:

$$\dot{\tilde{\boldsymbol{x}}}(t)=\boldsymbol{A}\tilde{\boldsymbol{x}}(t)+\boldsymbol{B}u(t)+\boldsymbol{L}(y(t)-\boldsymbol{C}\tilde{\boldsymbol{x}}(t)) \tag{3}$$

where $\tilde{\boldsymbol{x}}(t)=[\tilde{x}_1(t),\tilde{x}_2(t),\cdots,\tilde{x}_n(t)]^{\mathrm{T}}$. Define $\boldsymbol{e}(t)=\boldsymbol{x}(t)-\tilde{\boldsymbol{x}}(t)$. We can get the following error system:

$$\dot{\boldsymbol{e}}(t)=\tilde{\boldsymbol{A}}\boldsymbol{e}(t)+\boldsymbol{B}\varphi(t,x) \tag{4}$$

where $\tilde{\boldsymbol{A}}=\boldsymbol{A}-\boldsymbol{L}\boldsymbol{C}$ is Hurwitz. For the error system (4), we define the output signal $e_y(t)=y(t)-\boldsymbol{C}\hat{\boldsymbol{x}}(t)=\boldsymbol{C}\boldsymbol{e}(t)$. Then, the error system (4) with $e_y(t)$ as the output can be rewritten as

$$\begin{cases}\dot{\boldsymbol{e}}(t)=\tilde{\boldsymbol{A}}\boldsymbol{e}(t)+\boldsymbol{B}\varphi(t,\boldsymbol{x})\\ e_y(t)=\boldsymbol{C}\boldsymbol{e}(t)\end{cases}. \tag{5}$$

For system (5), the following proposition can be obtained.

Proposition 1 For system (1) under Assumption 2, if the LO is designed as (3) with $\tilde{\boldsymbol{A}}$ being Hurwitz, then the error system (5) is strongly observable.

Proof Note that the relative degree Assumption 2 implies that

$$\begin{cases}\boldsymbol{C}\boldsymbol{A}^i\boldsymbol{B}=\boldsymbol{0}, \quad i=0,1,\cdots,n-2\\ \boldsymbol{C}\boldsymbol{A}^{n-1}\boldsymbol{B}\neq\boldsymbol{0}\end{cases}. \tag{6}$$

By using $\boldsymbol{C}\boldsymbol{B}=\boldsymbol{0}$, it can be verified that

$$\boldsymbol{C}\tilde{\boldsymbol{A}}^i\boldsymbol{B}=\boldsymbol{C}\tilde{\boldsymbol{A}}^{i-1}(\boldsymbol{A}-\boldsymbol{L}\boldsymbol{C})\boldsymbol{B}=$$
$$\boldsymbol{C}\tilde{\boldsymbol{A}}^{i-1}\boldsymbol{A}\boldsymbol{B}-\boldsymbol{C}\tilde{\boldsymbol{A}}^{i-1}\boldsymbol{L}\boldsymbol{C}\boldsymbol{B}=\boldsymbol{C}\tilde{\boldsymbol{A}}^{i-1}\boldsymbol{A}\boldsymbol{B}. \tag{7}$$

By using $\boldsymbol{C}\boldsymbol{A}\boldsymbol{B}=\boldsymbol{0}$, (7) can be further simplified as

$$\boldsymbol{C}\tilde{\boldsymbol{A}}^i\boldsymbol{B}=\boldsymbol{C}\tilde{\boldsymbol{A}}^{i-1}\boldsymbol{A}\boldsymbol{B}=\boldsymbol{C}\tilde{\boldsymbol{A}}^{i-2}(\boldsymbol{A}-\boldsymbol{L}\boldsymbol{C})\boldsymbol{A}\boldsymbol{B}=$$
$$\boldsymbol{C}\tilde{\boldsymbol{A}}^{i-2}\boldsymbol{A}^2\boldsymbol{B}-\boldsymbol{C}\tilde{\boldsymbol{A}}^{i-2}\boldsymbol{L}\boldsymbol{C}\boldsymbol{A}\boldsymbol{B}=\boldsymbol{C}\tilde{\boldsymbol{A}}^{i-2}\boldsymbol{A}^2\boldsymbol{B}. \tag{8}$$

Following the same line of the calculation of (7)−(8), it can be finally calculated by using $\boldsymbol{C}\boldsymbol{A}^i\boldsymbol{B}=\boldsymbol{0}(i=0,1,\cdots,n-2)$ that

$$\boldsymbol{C}\tilde{\boldsymbol{A}}^i\boldsymbol{B}=\boldsymbol{C}\boldsymbol{A}^i\boldsymbol{B}. \tag{9}$$

It follows from (6) and (9) that

$$\begin{cases}\boldsymbol{C}\tilde{\boldsymbol{A}}^i\boldsymbol{B}=\boldsymbol{C}\boldsymbol{A}^i\boldsymbol{B}=\boldsymbol{0}, \quad i=0,1,\cdots,n-2\\ \boldsymbol{C}\tilde{\boldsymbol{A}}^{n-1}\boldsymbol{B}=\boldsymbol{C}\boldsymbol{A}^{n-1}\boldsymbol{B}\neq\boldsymbol{0}\end{cases} \tag{10}$$

which means that the relative degree of $e_y(t)$ with respect to the uncertainty $\varphi(t,\boldsymbol{x})$ is n. Hence, the proof is completed. □

(ii) Design of HOSMO

It is obvious that when $\varphi(t,\boldsymbol{x})=\boldsymbol{0}$, the observation error $\boldsymbol{e}(t)$ will converge to zero asymptotically. However, for the existence of uncertainty $\varphi(t,\boldsymbol{x})$, the error $\boldsymbol{e}(t)$ can only asymptotically converge to a bounded region. Moreover, our purpose is to develop a fixed-time observer, which cannot be achieved by the LO (3). In the following, a HOSMO will be constructed to solve this problem.

Under Proposition 1, we can always find a coordinate transformation $\bar{\boldsymbol{e}}(t)=[\bar{e}_1,\bar{e}_2,\cdots,\bar{e}_n]^{\mathrm{T}}=\boldsymbol{\varPhi}\boldsymbol{e}(t)$ with

$$\boldsymbol{\varPhi}=\begin{bmatrix}0&0&\cdots&0&1\\0&0&\cdots&1&\alpha_1\\\vdots&\vdots&\ddots&\vdots&\vdots\\1&\alpha_1&\cdots&\alpha_{n-2}&\alpha_{n-1}\end{bmatrix}\begin{bmatrix}\boldsymbol{C}\tilde{\boldsymbol{A}}^{n-1}\\\boldsymbol{C}\tilde{\boldsymbol{A}}^{n-2}\\\vdots\\\boldsymbol{C}\tilde{\boldsymbol{A}}^{0}\end{bmatrix} \tag{11}$$

such that the error system (5) can be transformed as

$$\begin{cases}\dot{\bar{\boldsymbol{e}}}(t)=\bar{\boldsymbol{A}}\bar{\boldsymbol{e}}(t)+\bar{\boldsymbol{B}}\varphi(t,\boldsymbol{x})\\ \bar{e}_y(t)=\bar{\boldsymbol{C}}\bar{\boldsymbol{e}}(t)\end{cases} \tag{12}$$

where the matrices $\bar{\boldsymbol{A}},\bar{\boldsymbol{B}},\bar{\boldsymbol{C}}$ are defined as

$$\bar{\boldsymbol{A}}=\boldsymbol{\varPhi}\tilde{\boldsymbol{A}}\boldsymbol{\varPhi}^{-1}=\begin{bmatrix}-[\alpha_1,\alpha_2,\cdots,\alpha_{n-1}]^{\mathrm{T}} & \boldsymbol{I}_{n-1}\\ -\alpha_n & \boldsymbol{0}_{1\times(n-1)}\end{bmatrix},$$

$$\bar{\boldsymbol{B}}=\boldsymbol{\varPhi}\boldsymbol{B}=[0,\cdots,0,\bar{\boldsymbol{C}}\tilde{\boldsymbol{A}}^{n-1}\boldsymbol{B}]^{\mathrm{T}},$$

$$\bar{\boldsymbol{C}}=\boldsymbol{C}\boldsymbol{\varPhi}^{-1}=[1,0,\cdots,0],$$

and $\alpha_1,\alpha_2,\cdots,\alpha_n$ are coefficients of $\det(s\boldsymbol{I}-\tilde{\boldsymbol{A}})=s^n+\alpha_1 s^{n-1}+\cdots+\alpha_{n-1}s+\alpha_n$.

Then, the following HOSMO can be designed:

$$\begin{cases}\dot{z}_1=v_0-k_1(1-\theta(t))\lceil\tilde{z}_1\rfloor^{\frac{n+1+\alpha}{n+1}}-\alpha_1\bar{e}_y(t)\\ v_0=-\kappa_1\varGamma^{\frac{1}{n+1}}\theta(t)\lceil\tilde{z}_1\rfloor^{\frac{n}{n+1}}+z_2\\ \dot{z}_i=v_{i-1}-k_i(1-\theta(t))\lceil\tilde{z}_1\rfloor^{\frac{n+1+\alpha i}{n+1}}-\alpha_i\bar{e}_y(t)\\ v_{i-1}=-\kappa_i\varGamma^{\frac{1}{n+2-i}}\theta(t)\lceil z_i-v_{i-2}\rfloor^{\frac{n-i+1}{n-i+2}}+z_{i+1}\\ \dot{z}_{n+1}=-\kappa_{n+1}\varGamma\theta(t)\mathrm{sign}(z_{n+1}-v_{n-1})-k_{n+1}(1-\theta(t))\lceil\tilde{z}_1\rfloor^{1+\alpha}\end{cases} \tag{13}$$

where $i=2,3,\cdots,n$, $z(t)=[z_1,z_2,\cdots,z_{n+1}]^{\mathrm{T}}$, $\tilde{z}_1=z_1-\bar{e}_1$, $\theta(t)=\dfrac{1}{2}(1+\mathrm{sign}(t-T_u))$ with $T_u>0$, and the parameters $\varGamma,\alpha>0$ and $\{\kappa_i,k_i\}_{i=1}^{n+1}$ will be given later.

(iii) Estimation of system state and uncertainty

Based on the proposed observer consisting of (3) and (13), the estimation of the system uncertainty and state is given as

$$\begin{cases}\hat{\boldsymbol{x}} = \tilde{\boldsymbol{x}}(t) + \boldsymbol{\Phi}^{-1}[z_1, z_2, \cdots, z_n]^{\mathrm{T}} \\ \hat{\varphi} = \left((\bar{\boldsymbol{C}}\tilde{\boldsymbol{A}}^{n-1}\boldsymbol{B})^{\mathrm{T}}(\bar{\boldsymbol{C}}\tilde{\boldsymbol{A}}^{n-1}\boldsymbol{B})\right)^{-1}(\bar{\boldsymbol{C}}\tilde{\boldsymbol{A}}^{n-1}\boldsymbol{B})^{\mathrm{T}} z_{n+1}\end{cases} \tag{14}$$

where $\tilde{\boldsymbol{x}}(t)$ is defined in (3); $z_1, z_2, \cdots, z_{n+1}$ are the states of HOSMO defined in (13); $\boldsymbol{\Phi}$ is the coordinate transformation matrix defined in (11).

3.2 Controller design

With the following coordinate transformation:

$$\boldsymbol{S} = \boldsymbol{\Psi}\boldsymbol{x} = [s_1, s_2, \cdots, s_n]^{\mathrm{T}},$$
$$\boldsymbol{\Psi} = [\boldsymbol{A}^{n-1}\boldsymbol{B}, \boldsymbol{A}^{n-2}\boldsymbol{B}, \cdots, \boldsymbol{A}\boldsymbol{B}, \boldsymbol{B}]^{-1},$$

we can obtain the following transformed system:

$$\begin{cases}\dot{s}_1 = s_2 \\ \quad\vdots \\ \dot{s}_{n-1} = s_n \\ \dot{s}_n = u + \varphi(t, x) + \displaystyle\sum_{i=1}^{n} a_i s_i\end{cases} \tag{15}$$

where a_i is determined by the coordinate transformation.

Note that $\tilde{\boldsymbol{x}}$ is unmeasurable. Therefore, $\boldsymbol{S} = \boldsymbol{\Psi}\boldsymbol{x}$ is also not available. With the help of the estimation $\hat{\boldsymbol{x}}$ defined in (14), we define

$$\begin{cases}\hat{\boldsymbol{S}} = \boldsymbol{\Psi}\hat{\boldsymbol{x}} = [\hat{s}_1, \hat{s}_2, \cdots, \hat{s}_n]^{\mathrm{T}} \\ \boldsymbol{\Psi} = [\boldsymbol{A}^{n-1}\boldsymbol{B}, \boldsymbol{A}^{n-2}\boldsymbol{B}, \cdots, \boldsymbol{A}\boldsymbol{B}, \boldsymbol{B}]^{-1}\end{cases}. \tag{16}$$

Then, the output-feedback controller can be designed as

$$u = -\sum_{i=1}^{n} \hbar_i |\hat{s}_i|^{\rho_i} \mathrm{sign}(\hat{s}_i) - \sum_{i=1}^{n} \bar{\hbar}_i |\hat{s}_i|^{\bar{\rho}_i} \mathrm{sign}(\hat{s}_i) - \hat{\varphi} - \sum_{i=1}^{n} a_i \hat{s}_i \tag{17}$$

where $\hat{s}_i (i = 1, 2, \cdots, n)$ is defined in (16) with $\hat{\boldsymbol{x}}, \hat{\varphi}$ defined in (14), and $\left\{\hbar_i, \bar{\hbar}_i, \rho_i, \bar{\rho}_i\right\}_{i=1}^{n}$ will be given later.

3.3 Main results

Following the design process of Subsection 3.1 to Subsection 3.2, we can finally construct an observer-based output feedback controller whose controller design block diagram is given in Fig. 1. In this subsection, the stability analysis of the closed-loop system is given in the following theorem which is the main result of this paper.

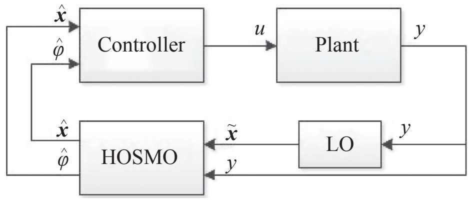

Fig. 1 Controller design block diagram

Theorem 1 Consider system (1) under Assumption 1 and Assumption 2. The observer is designed as (3)–(13), and the controller is designed as (17). Then, the closed-loop system is GFxTS if

(i) For (3), we select $\boldsymbol{L}$ such that $\boldsymbol{A} - \boldsymbol{LC}$ is Hurwitz;

(ii) For (13), we select $\varGamma$ such that $\varGamma \geqslant \|\bar{\boldsymbol{C}}\tilde{\boldsymbol{A}}^{n-1}\boldsymbol{B}\|\varphi_{\max}$, $\{\kappa_i\}_{i=1}^{n+1}$ in accordance with [6], $\{k_i\}_{i=1}^{n+1}$ such that $s^{n+1} + k_1 s^n + \cdots + k_n s + k_{n+1}$ is Hurwitz and $\alpha > 0$ being small enough;

(iii) For (17), we select the parameters $\left\{\hbar_i, \bar{\hbar}_i\right\}_{i=1}^{n}$ such that $s^n + \hbar_n s^{n-1} + \cdots + \hbar_2 s + \hbar_1$ and $s^n + \bar{\hbar}_n s^{n-1} + \cdots + \bar{\hbar}_2 s + \bar{\hbar}_1$ are Hurwitz, $\{\rho_i, \bar{\rho}_i\}_{i=1}^{n}$ according to

$$\begin{cases}\rho_{i-1} = \dfrac{\rho_i \rho_{i+1}}{2\rho_{i+1} - \rho_i} \\ \bar{\rho}_{i-1} = \dfrac{\bar{\rho}_i \bar{\rho}_{i+1}}{2\bar{\rho}_{i+1} - \bar{\rho}_i}\end{cases}, \quad i = 2, 3, \cdots, n \tag{18}$$

where $\rho_{n+1} = \bar{\rho}_{n+1} = 1$, $\rho_n = \rho_0 \in (1 - \varepsilon, 1)$ and $\bar{\rho}_n = \bar{\rho}_0 \in (1, 1 + \varepsilon)$ with $\varepsilon > 0$ being sufficiently small.

Proof For the HOSMO (13), we define the observation error variables $\tilde{z}_i = z_i - \bar{e}_i$ for $i = 1, 2, \cdots, n$ and $\tilde{z}_{n+1} = z_{n+1} - \bar{\boldsymbol{C}}\tilde{\boldsymbol{A}}^{n-1}\boldsymbol{B}\varphi(t, \boldsymbol{x})$. Then, with (12) and (13), one can get the following error system:

$$\begin{cases}\dot{\tilde{z}}_1 = -\kappa_1 \varGamma^{\frac{1}{n+1}} \theta(t) \lceil \tilde{z}_1 \rfloor^{\frac{n}{n+1}} - k_1(1 - \theta(t)) \lceil \tilde{z}_1 \rfloor^{\frac{n+1+\alpha}{n+1}} + \tilde{z}_2 \\ \dot{\tilde{z}}_i = -\kappa_i \varGamma^{\frac{1}{n+2-i}} \theta(t) \lceil z_i - v_{i-2} \rfloor^{\frac{n-i+1}{n-i+2}} - \\ \qquad k_i(1 - \theta(t)) \lceil \tilde{z}_1 \rfloor^{\frac{n+1+\alpha i}{n+1}} + \tilde{z}_{i+1}, \quad i = 2, 3, \cdots, n \\ \dot{\tilde{z}}_{n+1} = -\kappa_{n+1} \varGamma \theta(t) \mathrm{sign}(z_{n+1} - v_{n-1}) - \\ \qquad k_{n+1}(1 - \theta(t)) \lceil \tilde{z}_1 \rfloor^{1+\alpha} - \bar{\boldsymbol{C}}\tilde{\boldsymbol{A}}^{n-1}\boldsymbol{B}\dot{\varphi}(t, x)\end{cases} \tag{19}$$

where $v_0, v_1, \cdots, v_{n-1}$ are defined in (13) and rewritten as

$$\begin{cases}v_0 = -\kappa_1 \varGamma^{\frac{1}{n+1}} \theta(t) \lceil \tilde{z}_1 \rfloor^{\frac{n}{n+1}} + z_2 \\ v_1 = -\kappa_2 \varGamma^{\frac{1}{n}} \theta(t) \lceil z_2 - v_0 \rfloor^{\frac{n-1}{n}} + z_3 \\ \quad\vdots \\ v_{n-1} = -\kappa_n \varGamma^{\frac{1}{2}} \theta(t) \lceil z_n - v_{n-2} \rfloor^{\frac{1}{2}} + z_{n+1}\end{cases}. \tag{20}$$

(i) In the following, we will first prove that the error system (19) is GFxTS.

Case $t \leqslant T_u$: When $t \leqslant T_u$, we have $\theta(t) = 0$. Then, the error system (19) will reduce to

$$\begin{cases}\dot{\tilde{z}}_1 = -k_1\lceil \tilde{z}_1 \rfloor^{\frac{n+1+\alpha}{n+1}} + \tilde{z}_2 \\ \dot{\tilde{z}}_2 = -k_2\lceil \tilde{z}_1 \rfloor^{\frac{n+1+2\alpha}{n+1}} + \tilde{z}_3 \\ \quad\vdots \\ \dot{\tilde{z}}_n = -k_n\lceil \tilde{z}_1 \rfloor^{\frac{n+1+n\alpha}{n+1}} + \tilde{z}_{n+1} \\ \dot{\tilde{z}}_{n+1} = -k_{n+1}\lceil \tilde{z}_1 \rfloor^{1+\alpha} - \bar{\boldsymbol{C}}\tilde{\boldsymbol{A}}^{n-1}\boldsymbol{B}\dot{\varphi}(t,\boldsymbol{x})\end{cases} \tag{21}$$

where $\tilde{z}(t) = [\tilde{z}_1, \tilde{z}_2, \cdots, \tilde{z}_{n+1}]^{\mathrm{T}}$. For system (21), we can obtain the following three properties:

i) According to [18], when $\bar{\boldsymbol{C}}\tilde{\boldsymbol{A}}^{n-1}\boldsymbol{B}\dot{\varphi}(t,\boldsymbol{x}) = 0$, the origin of system (21) is globally asymptotically stable;

ii) According to Definition 3, when $\bar{\boldsymbol{C}}\tilde{\boldsymbol{A}}^{n-1}\boldsymbol{B}\dot{\varphi}(t,\boldsymbol{x}) = 0$, the right side of system (21) is r-homogeneous with homogeneity degree α, where $\boldsymbol{r} = [r_1, r_2, \cdots, r_{n+1}]^{\mathrm{T}}$ with $r_i = n+1+\alpha(i-1)(i = 1,2,\cdots,n+1)$;

iii) According to Assumption 1, $\bar{\boldsymbol{C}}\tilde{\boldsymbol{A}}^{n-1}\boldsymbol{B}\dot{\varphi}(t,\boldsymbol{x})$ is uniformly bounded by $\|\bar{\boldsymbol{C}}\tilde{\boldsymbol{A}}^{n-1}\boldsymbol{B}\|\varphi_{\max}$.

It follows from Definition 2 and Lemma 1 of [34] that system (21) is GPFxTS. Moreover, with Lemma 3 of [34], we can also conclude that for any given time $T_u \geqslant 0$, there exists a constant δ such that any solution of system (21) satisfies $\|\tilde{z}(t)\| \leqslant \delta$ for $\forall t \geqslant T_u$.

Case $t > T_u$: When $t > T_u$, we have $\theta(t) = 1$. Then, the error system (19) will reduce to

$$\begin{cases}\dot{\tilde{z}}_1 = -\kappa_1\Gamma^{\frac{1}{n+1}}\lceil \tilde{z}_1 \rfloor^{\frac{n}{n+1}} + \tilde{z}_2 \\ \dot{\tilde{z}}_2 = -\kappa_2\Gamma^{\frac{1}{n}}\lceil z_2 - v_0 \rfloor^{\frac{n-1}{n}} + \tilde{z}_3 \\ \quad\vdots \\ \dot{\tilde{z}}_n = -\kappa_n\Gamma^{\frac{1}{2}}\lceil z_n - v_{n-2} \rfloor^{\frac{1}{2}} + \tilde{z}_{n+1} \\ \dot{\tilde{z}}_{n+1} = -\kappa_{n+1}\Gamma\operatorname{sign}(z_{n+1} - v_{n-1}) - \bar{\boldsymbol{C}}\tilde{\boldsymbol{A}}^{n-1}\boldsymbol{B}\dot{\varphi}(t,\boldsymbol{x})\end{cases} \tag{22}$$

where $v_0, v_1, \cdots, v_{n-1}$ are defined in (20). Define $\bar{z}_i = \tilde{z}_i/\Gamma$ $(i = 1,2,\cdots,n+1)$. Then, the derivative of $\bar{z}_1$ can be calculated as

$$\dot{\bar{z}}_1 = -\kappa_1\lceil \bar{z}_1 \rfloor^{\frac{n}{n+1}} + \bar{z}_2. \tag{23}$$

Similarly, the derivative of $\bar{z}_2$ can be calculated as

$$\dot{\bar{z}}_2 = \frac{-\kappa_2\Gamma^{\frac{1}{n}}\lceil z_2 - v_0 \rfloor^{\frac{n-1}{n}} + \tilde{z}_3}{\Gamma} = -\frac{\kappa_2\Gamma^{\frac{1}{n}}\lceil z_2 - v_0 \rfloor^{\frac{n-1}{n}}}{\Gamma} + \bar{z}_3. \tag{24}$$

It follows from (20) and (23) that

$$z_2 - v_0 = \kappa_1\Gamma^{\frac{1}{n+1}}\lceil \bar{z}_1 \rfloor^{\frac{n}{n+1}} = \kappa_1\Gamma\lceil \bar{z}_1 \rfloor^{\frac{n}{n+1}} = \Gamma(\bar{z}_2 - \dot{\bar{z}}_1), \tag{25}$$

which implies that

$$\dot{\bar{z}}_2 = -\kappa_2\lceil \bar{z}_2 - \dot{\bar{z}}_1 \rfloor^{\frac{n-1}{n}} + \bar{z}_3. \tag{26}$$

Following the same way to get (25) and (26), we have

$$z_i - v_{i-2} = \Gamma(\bar{z}_i - \dot{\bar{z}}_{i-1}), \quad i = 1,2,\cdots,n \tag{27}$$

and

$$\dot{\bar{z}}_i = -\kappa_i\lceil \bar{z}_i - \dot{\bar{z}}_{i-1} \rfloor^{\frac{n-i+1}{n-i+2}} + \bar{z}_{i+1}, \quad i = 1,2,\cdots,n. \tag{28}$$

Finally, it can be calculated from (20), (27) and (28) that

$$z_{n+1} - v_{n-1} = \kappa_n\Gamma^{\frac{1}{2}}\lceil z_n - v_{n-2} \rfloor^{\frac{1}{2}} = \kappa_n\Gamma\lceil \bar{z}_n - \dot{\bar{z}}_{n-1} \rfloor^{\frac{1}{2}} = \Gamma(\bar{z}_{n+1} - \dot{\bar{z}}_n). \tag{29}$$

Then, the following differential inclusion can be obtained:

$$\dot{\bar{z}}_{n+1} = \frac{-\kappa_{n+1}\Gamma\operatorname{sign}(z_{n+1} - v_{n-1}) - \boldsymbol{C}\tilde{\boldsymbol{A}}^{n-1}\boldsymbol{B}\dot{\varphi}(t,\boldsymbol{x})}{\Gamma} = -\kappa_{n+1}\operatorname{sign}(\bar{z}_{n+1} - \dot{\bar{z}}_n) - \frac{\boldsymbol{C}\tilde{\boldsymbol{A}}^{n-1}\boldsymbol{B}\dot{\varphi}(t,\boldsymbol{x})}{\Gamma} \in -\kappa_{n+1}\operatorname{sign}(\bar{z}_{n+1} - \dot{\bar{z}}_n) + [-1,1], \tag{30}$$

which is understood in the Filippov sense [33].

Putting (23), (26), (28) and (30) together, we have

$$\begin{cases}\dot{\bar{z}}_1 = -\kappa_1\lceil \bar{z}_1 \rfloor^{\frac{n}{n+1}} + \bar{z}_2 \\ \dot{\bar{z}}_2 = -\kappa_2\lceil \bar{z}_2 - \dot{\bar{z}}_1 \rfloor^{\frac{n-1}{n}} + \bar{z}_3 \\ \quad\vdots \\ \dot{\bar{z}}_n = -\kappa_n\lceil \bar{z}_n - \dot{\bar{z}}_{n-1} \rfloor^{\frac{1}{2}} + \bar{z}_{n+1} \\ \dot{\bar{z}}_{n+1} \in -\kappa_{n+1}\operatorname{sign}(\bar{z}_{n+1} - \dot{\bar{z}}_n) + [-1,1]\end{cases} \tag{31}$$

where $\bar{z}(t) = [\bar{z}_1, \bar{z}_2, \cdots, \bar{z}_{n+1}]^{\mathrm{T}}$. It follows from Theorem 5 of [6] that $\bar{z}(t)$ and thus $\tilde{z}(t)$ will convergence to zero in a finite time whose convergence time is dependent on the initial value $\bar{z}(T_u)$.

Note that the error system (19) will take the form as (21) for $t \leqslant T_u$ and (22) for $t > T_u$. It has been proved in the condition Case $t \leqslant T_u$ that $\|\tilde{z}(T_u)\| \leqslant \delta$ and thus $\|\bar{z}(T_u)\| \leqslant \delta/\Gamma$. Since the convergence time of system (31) depends on the system initial value $\tilde{z}(T_u)$ which is bounded by a constant δ/Γ, the convergence time of system (31) is also uniformly bounded by some constant $\bar{T}_1^{\max}$. Therefore, the convergence time of system (19) is uniformly bounded by some constant $T_{\max}^1 = T_u + \bar{T}_1^{\max}$, which implies that system (19) is GFxTS, i.e., $\tilde{z}(t) = \mathbf{0}$ holds for $\forall t \geqslant T_{\max}^1$.

(ii) Then, we will prove that the system uncertainty $\varphi(t,\boldsymbol{x})$ and state $\boldsymbol{x}(t)$ can be fixed-time estimated by $\hat{\boldsymbol{x}}, \hat{\varphi}$.

In the above, we have proven that there exists a fixed-time $T_{\max}^1$ independent of the system initial values such that $\tilde{z}(t) = \mathbf{0}$ holds for $\forall t \geqslant T_{\max}^1$. Note that $\tilde{z}(t) = \mathbf{0}$, $t \geqslant T_{\max}^1$ means that the following equations hold:

$$\begin{cases} z_i = \bar{e}_i, \quad i = 1,2,\cdots,n \\ z_{n+1} = \bar{\boldsymbol{C}}\tilde{\boldsymbol{A}}^{n-1}\boldsymbol{B}\varphi(t,\boldsymbol{x}) \end{cases} \tag{32}$$

for $\forall t \geqslant T_{\max}^1$. When $t \geqslant T_{\max}^1$, it follows from (14) and (32) that

$$\begin{aligned} \hat{\boldsymbol{x}} &= \tilde{\boldsymbol{x}}(t) + \boldsymbol{\Phi}^{-1}[z_1, z_2, \cdots, z_n]^{\mathrm{T}} = \\ &\tilde{\boldsymbol{x}}(t) + \boldsymbol{\Phi}^{-1}[\bar{e}_1, \bar{e}_2, \cdots, \bar{e}_n]^{\mathrm{T}} = \tilde{\boldsymbol{x}}(t) + \boldsymbol{\Phi}^{-1}\bar{\boldsymbol{e}}(t) \end{aligned} \tag{33}$$

holds for $\forall t \geqslant T_{\max}^1$. Note that $\boldsymbol{e}(t) = \boldsymbol{x}(t) - \tilde{\boldsymbol{x}}(t)$ implies that $\tilde{\boldsymbol{x}}(t) = \boldsymbol{x}(t) - \boldsymbol{e}(t)$. Also note that $\bar{\boldsymbol{e}}(t) = \boldsymbol{\Phi}\boldsymbol{e}(t)$. Substituting the above two equations into (33), we have

$$\hat{\boldsymbol{x}} = \boldsymbol{x}(t) - \boldsymbol{e}(t) + \boldsymbol{\Phi}^{-1}\boldsymbol{\Phi}\boldsymbol{e}(t) = \boldsymbol{x}(t) \tag{34}$$

holds for $\forall t \geqslant T_{\max}^1$. Similarly, we can also obtain from (14) and (32) that

$$\begin{aligned} \hat{\varphi} &= \left((\bar{\boldsymbol{C}}\tilde{\boldsymbol{A}}^{n-1}\boldsymbol{B})^{\mathrm{T}}(\bar{\boldsymbol{C}}\tilde{\boldsymbol{A}}^{n-1}\boldsymbol{B})\right)^{-1} \cdot \\ &(\bar{\boldsymbol{C}}\tilde{\boldsymbol{A}}^{n-1}\boldsymbol{B})^{\mathrm{T}}(\bar{\boldsymbol{C}}\tilde{\boldsymbol{A}}^{n-1}\boldsymbol{B})\varphi(t,\boldsymbol{x}) = \varphi(t,\boldsymbol{x}) \end{aligned} \tag{35}$$

holds for $\forall t \geqslant T_{\max}^1$. Therefore, it can be concluded from (34) and (35) that the system uncertainty $\varphi(t,\boldsymbol{x})$ and state $\boldsymbol{x}(t)$ can be fixed-time estimated by $\hat{\boldsymbol{x}}, \hat{\varphi}$.

(iii) Finally, we will show that the closed-loop system composed of (1), (3), (13) and (17) is GFxTS.

It has been proved in the previous that $\boldsymbol{x}(t) = \hat{\boldsymbol{x}}$, $\varphi(t,\boldsymbol{x}) = \hat{\varphi}$ hold for $\forall t \geqslant T_{\max}^1$, which means that $\hat{s}_i = s_i (i = 1,2,\cdots,n), \forall t \geqslant T_{\max}^1$. In this case, system (15) will reduce to

$$\begin{cases} \dot{s}_i = s_{i+1}, \quad i = 1,2,\cdots,n-1 \\ \dot{s}_n = -\sum\limits_{i=1}^{n} \hbar_i |s_i|^{\rho_i}\mathrm{sign}(s_i) - \sum\limits_{i=1}^{n} \bar{\hbar}_i |s_i|^{\bar{\rho}_i}\mathrm{sign}(s_i) \end{cases}. \tag{36}$$

It follows from Theorem 2 of [24] that system (36) is GFxTS, i.e., there exists a fixed time $T_{\max}^2$ free of the system initial conditions such that $s_i = 0 (i = 1,2,\cdots,n)$ holds for $\forall t \geqslant T_{\max}^1 + T_{\max}^2 = T_{\max}$. Note that $s_i = 0\ (i = 1,2,\cdots,n)$ means that $\boldsymbol{x}(t) \equiv \mathbf{0}$. Therefore, the closed-loop system comosed of (1), (3), (13) and (17) is GFxTS. □

Remark 2 Note that the observer designed in this paper is similar to that in [11−13]. However, all the observers in [11−13] is finite-time stable with convergence time depending on the system initial error conditions. Therefore, the observers in [11−13] cannot be used in this paper. Also note that most of the existing fixed-time observers [29−31] can only identify the system states. The proposed observer in this paper can achieve fixed-time observation of the system states as well as the system uncertainties, simultaneously.

Remark 3 It can be clearly seen from Theorem 1 that the proposed observer-based controller can achieve stabilization of system (1) in a fixed-time independent of system initial conditions. Different from the existing fixed-time controller [26−28], the proposed controller is completely continuous and only needs the output signals for feedback.

Remark 4 In Theorem 1, the parameters $\{\kappa_i\}_{i=1}^{n+1}$ are selected according to the original HOSMO [6]. According to [6], possible choices of the parameters $\{\kappa_i\}_{i=1}^{n+1}$ for $n \leqslant 5$ are given as follows:

$$\begin{gathered} \{\kappa_i\}_{i=1}^2 = \{\kappa_2 = 1.1, \kappa_1 = 1.5\}, \\ \{\kappa_i\}_{i=1}^3 = \{\kappa_3 = 1.1, \kappa_2 = 1.5, \kappa_1 = 2\}, \\ \{\kappa_i\}_{i=1}^4 = \{\kappa_4 = 1.1, \kappa_3 = 1.5, \kappa_2 = 2, \kappa_1 = 3\}, \\ \{\kappa_i\}_{i=1}^5 = \{\kappa_5 = 1.1, \kappa_4 = 1.5, \kappa_3 = 2, \kappa_2 = 3, \kappa_1 = 5\}, \\ \{\kappa_i\}_{i=1}^6 = \{\kappa_6 = 1.1, \kappa_5 = 1.5, \kappa_4 = 2, \kappa_3 = 3, \kappa_2 = 5, \kappa_1 = 8\}. \end{gathered}$$

Remark 5 Note that the nonlinear items in the controller (17) are complex. Therefore, the boundedness of states over the time interval $[0, T_{\max}^1]$ is not proved here. One can set $u = u_1$ over the time interval $[0, T_{\max}^1]$, where u_1 is used to guarantee the boundedness of states for $t \in [0, T_{\max}^1]$. Generally, the controller u_1 can be simply set as $u_1 = 0$. Then, when $t > T_1^{\max}$, the controller can be switched from u_1 to (17). Therefore, the problem becomes that how to obtain the convergence time of the observer $T_{\max}^1$ in this paper. To solve this problem, we can detect the signal $e_y(t) = y(t) - \boldsymbol{C}\hat{\boldsymbol{x}}(t)$ online. Define a small positive constant $\Delta T > 0$. If for some time instant $t = T$, we have $e_y(T) = 0$ and $e_y(t) = 0$ still holds for $t \in (T, T + \Delta T]$, then we can set $T_{\max}^1 = T + \Delta T$. It should be pointed out that in practice, for the existence of sampling time, measurement noise and many other factors, the exact observation $e_y(t) = 0$ cannot be achieved. To overcome the problem, we can use $\|e_y(t)\| \leqslant \varsigma$ to replace $e_y(t) = 0$, where $\varsigma > 0$ is a constant to be chosen small enough.

Remark 6 Also note that for LO (3) and HOSMO (13), the errors between $\boldsymbol{x}(t), \varphi(t,\boldsymbol{x})$ and $\hat{\boldsymbol{x}}, \hat{\boldsymbol{\varphi}}$ may be very large at the initial stage of the time interval $[0, T_{\max}^1]$. In this case, if we use the estimated variables $\hat{\boldsymbol{x}}, \hat{\boldsymbol{\varphi}}$ directly in the controller, a peaking problem may be caused. This problem can also be solved by redesigning the controller $u = u_1$ over the time interval $[0, T_{\max}^1]$. Actually, in most cases, by simply setting $u_1 = 0$, the peaking problem can be greatly reduced.

4. Simulation

In the simulation, we consider the following system:

$$\begin{cases} \dot{\boldsymbol{x}}(t) = \boldsymbol{A}\boldsymbol{x}(t) + \boldsymbol{B}(u + d(t)) \\ y(t) = \boldsymbol{C}\boldsymbol{x}(t) \end{cases} \tag{37}$$

where $\boldsymbol{A} = \begin{bmatrix} 0 & 1 \\ -1 & 1 \end{bmatrix}, \boldsymbol{B} = [0,1]^{\mathrm{T}}, \boldsymbol{C} = [1,0]$, and $d(t)$ is the matched disturbance selected as $d(t) = 5 + 2\cos(2t+1)$.

In the following, different control schemes will be used to make simulation comparison.

4.1 Design of controllers

In the following, the control schemes proposed in this paper and [19] will be applied to design the controller and make simulation comparison.

(i) The proposed fixed-time output-feedback controller

At first, the control scheme proposed in this paper will be used to design the controller. According to Theorem 1, the composite observer can be designed for system (37) as

$$\dot{\tilde{\boldsymbol{x}}}(t) = \boldsymbol{A}\tilde{\boldsymbol{x}}(t) + \boldsymbol{B}u(t) + \boldsymbol{L}(y(t) - \boldsymbol{C}\tilde{\boldsymbol{x}}(t)),$$

$$\begin{cases} \dot{z}_1 = v_0 - k_1(1-\theta(t))\lceil \bar{z}_1 \rfloor^{\frac{3+\alpha}{3}} - \bar{e}_1 \\ v_0 = -\kappa_1 \Gamma^{\frac{1}{3}} \theta(t) \lceil \bar{z}_1 \rfloor^{\frac{2}{3}} + z_2 \\ \dot{z}_2 = v_1 - k_2(1-\theta(t))\lceil \bar{z}_1 \rfloor^{\frac{3+2\alpha}{3}} - \bar{e}_1 \\ v_1 = -\kappa_2 \Gamma^{\frac{1}{2}} \theta(t) \lceil z_2 - v_0 \rfloor^{\frac{1}{2}} + z_3 \\ \dot{z}_3 = -\kappa_3 \Gamma \theta(t) \mathrm{sign}(z_3 - v_1) - k_3(1-\theta(t))\lceil \bar{z}_1 \rfloor^{1+\alpha} \end{cases}, \tag{38}$$

where $\boldsymbol{L}$ is selected as $\boldsymbol{L} = [l_1, l_2]^{\mathrm{T}} = [2,2]^{\mathrm{T}}$, $\bar{\boldsymbol{e}}(t) = [\bar{e}_1, \bar{e}_2]^{\mathrm{T}}$ is defined as $\bar{\boldsymbol{e}}(t) = \boldsymbol{\Phi}\boldsymbol{e}(t)$ with $\boldsymbol{e}(t) = \boldsymbol{x}(t) - \tilde{\boldsymbol{x}}(t)$, $\boldsymbol{\Phi} = \begin{bmatrix} 1 & 0 \\ -1 & 1 \end{bmatrix}$ and $\theta(t) = (1+\mathrm{sign}(t - T_u))/2$ with $T_u = 2$, the parameters $\{k_i\}_{i=1}^3$, Γ and α are selected as $\kappa_1 = 2$, $\kappa_2 = 1.5, \kappa_3 = 1.1, k_1 = 7, k_2 = 2 + \dfrac{1}{7}, k_3 = 1, \Gamma = 10, \alpha = 0.06$.

Based on the composite observer, the system uncertainty $d(t)$ and state $\boldsymbol{x}(t)$ are estimated as

$$\begin{cases} \hat{\boldsymbol{x}} = [\hat{x}_1, \hat{x}_2]^{\mathrm{T}} = \tilde{\boldsymbol{x}}(t) + \boldsymbol{\Phi}^{-1}[z_1, z_2]^{\mathrm{T}} \\ \hat{d} = z_3 \end{cases}. \tag{39}$$

According to Theorem 1, the output-feedback fixed-time controller can be finally implemented as

$$\begin{gathered} u = -\hbar_1 |\hat{x}_1|^{\rho_1} \mathrm{sign}(\hat{x}_1) - \\ \hbar_2 |\hat{x}_2|^{\rho_2} \mathrm{sign}(\hat{x}_2) - \bar{\hbar}_1 |\hat{x}_1|^{\bar{\rho}_1} \mathrm{sign}(\hat{x}_1) - \\ \bar{\hbar}_2 |\hat{x}_2|^{\bar{\rho}_2} \mathrm{sign}(\hat{x}_2) - \hat{d} + \hat{x}_1 \end{gathered} \tag{40}$$

where the parameters are selected as $\hbar_1 = \hbar_2 = \bar{\hbar}_1 = \bar{\hbar}_2 = 4, \rho_1 = \dfrac{7}{9}, \rho_2 = \dfrac{7}{8}, \bar{\rho}_1 = \dfrac{9}{7}, \bar{\rho}_2 = \dfrac{9}{8}$.

(ii) Continuous fixed-time attractive controller [19]

Secondly, by using the estimated state given in (39), a fixed-time attractive controller can be designed according to Theorem 1 of [19] as

$$u = \hat{x}_1 - \hat{x}_2 - \alpha_1 \hat{x}_2 + 3\beta_1 \hat{x}_1^2 \hat{x}_2 - \alpha_2 s_2 - \beta_2 s_2^3 \tag{41}$$

where $s_1 = \hat{x}_1, s_2 = \hat{x}_2 + \alpha_1 \hat{x}_1 + \beta_1 \hat{x}_1^3$ with the parameters being selected as $\alpha_1 = \alpha_2 = \beta_1 = \beta_2 = 1$.

(iii) Discontinuous fixed-time controller [19]

Finally, by using the estimated state $\hat{\boldsymbol{x}}$, a discontinuous fixed-time controller is designed according to Theorem 2 of [19] as

$$u = \hat{x}_1 - \hat{x}_2 - (\alpha_1 + 3\beta_1 \hat{x}^2 + d_{\max})\mathrm{sign}(s) - \left\lceil \alpha_2 s + \beta_2 \lceil s \rfloor^3 \right\rfloor^{\frac{1}{2}} \tag{42}$$

where $s = \hat{x}_2 + \left\lceil \lceil \hat{x}_2 \rfloor^2 + \alpha_1 \hat{x}_1 + \beta_1 \lceil \hat{x}_1 \rfloor^3 \right\rfloor^{\frac{1}{2}}$ with the parameters being selected as $\alpha_1 = \alpha_2 = \beta_1 = \beta_2 = 1$ and $d_{\max} = 10$.

4.2 Simulation results

To make the simulation comparison, two different initial conditions for system (37) are selected as

$$\begin{cases} \text{(i)}: \ \boldsymbol{x}(0) = [0.5, 0.5]^{\mathrm{T}} \\ \text{(ii)}: \ \boldsymbol{x}(0) = [100, 100]^{\mathrm{T}} \end{cases}, \tag{43}$$

one of which is small and the other is large. The initial condition for observer (38) is selected as zero. Firstly, curves under the proposed composite observer (38) and controller (40) are given in Fig. 2. It can be concluded from Fig. 2 that the estimation errors and system states can be driven to zero with a fast speed and high precision even with different initial conditions. Moreover, the control signal is completely continuous and therefore is free of chattering. Secondly, curves under controllers (41) and (42) are given in Fig. 3 and Fig. 4 for comparison. It can be concluded from Fig. 3 and Fig. 4 that the system states can only be driven to a bounded region around origin while under controller (41), and while under controller (42) the system will suffer from serious chattering problem.

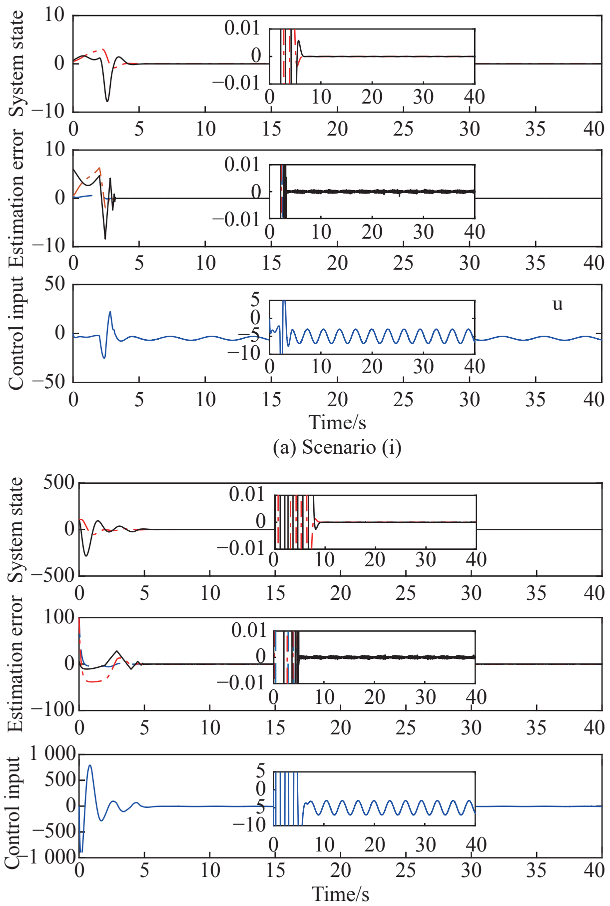

(a) Scenario (i)

(b) Scenario (ii)

$-\cdot-$: x_1; —— : x_2; $-\cdot$: $\hat{x}_1-x_1$; $-\cdot\cdot$: $\hat{x}_2-x_2$; —— : $\hat{d}-d$; —— : u.

Fig. 2 Curves under proposed fixed-time output-feedback controller (40)

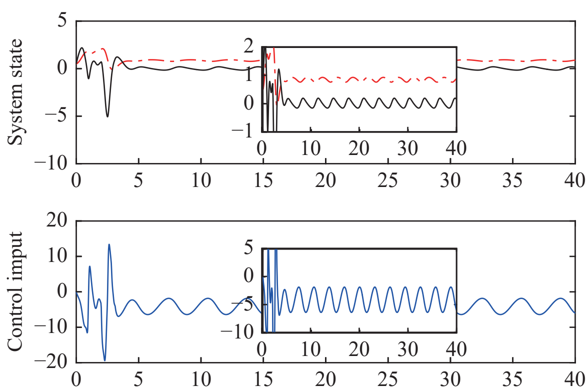

(a) Scenario (i)

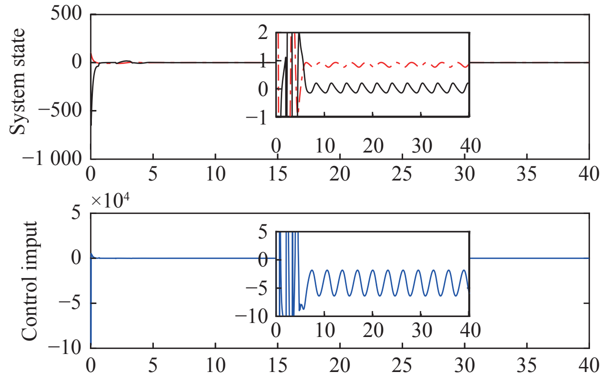

(b) Scenario (ii)

$-\cdot-$: x_1; —— : x_2; —— : u.

Fig. 3 Curves under the fixed-time attractive controller (41) proposed in [19]

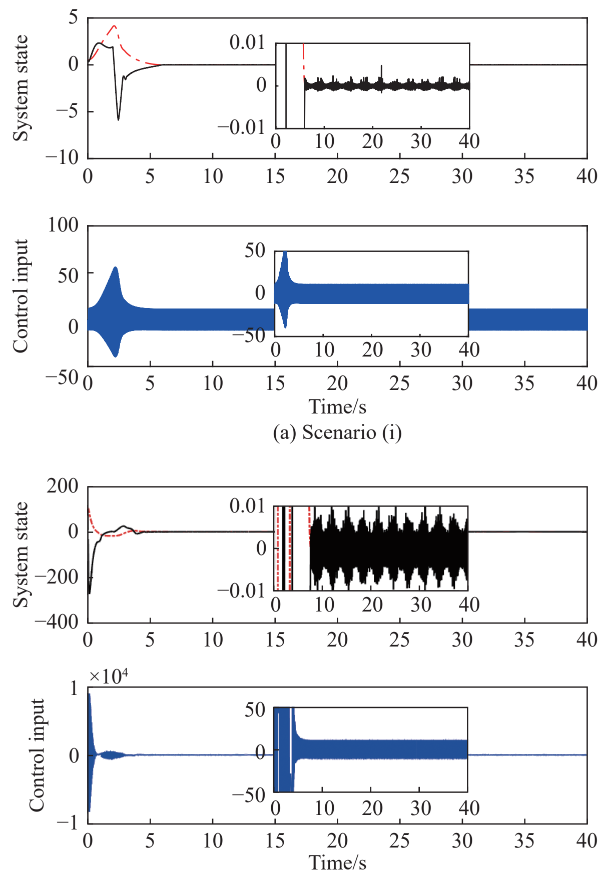

(a) Scenario (i)

(b) Scenario (ii)

$-\cdot-$: x_1; —— : x_2; —— : u.

Fig. 4 Curves under the discontinuous fixed-time controller (42) proposed in [19]

5. Conclusions

In this paper, a composite fixed-time observer-based output-feedback controller is developed for uncertain liner systems.

Firstly, we design a composite fixed-time observer. The composite fixed-time observer consists of a HOSMO and a LO. One remarkable property of the proposed observer is that it can achieve simultaneous exact observation of the uncertainties and states in fixed-time independent of system initial error conditions. Then, by using the uncertainty compensation method, a robust continuous output-feedback controller with fixed-time convergence guarantee and without chattering problem is constructed. Simulation comparison with existing continuous fixed-time attractive controller and discontinuous fixed-time controller is also given to show the advantages of the controller.

How to extend this result to more general multi-input and multi-output systems is our future work.

References

[1] GONG X, FU Y B, JIANG L X, et al. Application of super-twisting extended state observer in fault reconfiguration of quadrotor aircraft. Systems Engineering and Electronics, 2020, 42(9): 2077–2084. (in Chinese)

[2] ZHAO Y, DONG L L. Adaptive back-stepping control on container ships for path following. Journal of Systems Engineering and Electronics, 2020, 31(4): 780–791.

[3] MIN H F, XU S Y, ZHANG Z Q. Adaptive finite-time stabilization of stochastic nonlinear systems subject to full-state constraints and input saturation. IEEE Trans. on Automatic Control, 2021, 66(3): 1306–1313.

[4] MIN H F, XU S Y, ZHANG B Y, et al. Globally adaptive control for stochastic nonlinear time-delay systems with perturbations and its application. Automatica , 2019, 102: 105–110.

[5] UTKIN V, Sliding modes in control and optimization. Berlin: Springer-Verlag, 1992.

[6] LEVANT A. Higher-order sliding modes, differentiation and output-feedback control. International Journal of Control, 2003, 76(9/10): 924–941.

[7] DING S H, LEVANT A, LI S H. Simple homogeneous sliding-mode controller. Automatica, 2016, 67: 22–32.

[8] SHI S, XU S Y, GU J, et al. Global high-order sliding mode controller design subject to mismatched terms: application to buck converter. IEEE Trans. on Circuits Systems-I: Regular Papers, 2019, 66(12): 4840–4849.

[9] MIN H F, XU S Y, MA Q, et al. Composite-observer-based output-feedback control for nonlinear time-delay systems with input saturation and its application. IEEE Trans. on Industrial Electronics, 2018, 65(7): 5856–5863.

[10] MIN H F, XU S Y, ZHANG B Y, et al. Output-feedback control for stochastic nonlinear systems subject to input saturation and time-varying delay. IEEE Trans. on Automatic Control, 2018, 64(1): 359–364.

[11] BEJARANO F, FRIDMAN L, POZNYAK A. Exact state estimation for linear systems with unknown inputs based on hierarchical super-twisting algorithm. International Journal of Robust Nonlinear Control, 2007, 17(18): 1734–1753.

[12] LOZA A, BEJARANO F, FRIDMAN L. Unmatched uncertainties compensation based on high-order sliding mode observation. International Journal of Robust Nonlinear Control, 2013, 23(7): 754–764.

[13] FERREIRA A, BEJARANO F, FRIDMAN L. Robust control with exact uncertainties compensation: with or without chattering? IEEE Trans. on Control Systems Technology, 2011, 19(5): 965–975.

[14] BASIN M, PANATHULA C, SHTESSEL Y, et al. Continuous finite-time higher order output regulators for systems with unmatched unbounded disturbances. IEEE Trans. on Industrial Electronics, 2016, 63(8): 5036–5043.

[15] SHI S, XU S Y, YU X, et al. Robust output-feedback finite-time regulator of systems with mismatched uncertainties bounded by positive functions. IET Control Theory and Application, 2017, 11(17): 3107–3114.

[16] MIN H F, XU S Y, ZHANG B Y, et al. Practically finite-time control for nonlinear systems with mismatching conditions and application to a robot system. IEEE Trans. on Systems, Man, and Cybernetics: Systems, 2020, 50(2): 2168–2216.

[17] YANG R M, PEI W H, HAN Y Z, et al. Finite-time adaptive robust simultaneous stabilization of nonlinear delay systems by the Hamiltonian function method. Science China: Information Science, 2021, 64(6): 169201.

[18] ANDRIEU V, PRALY L, ASTOLFI A. Homogeneous approximation, recursive observer and output feedback. SIAM Journal on Control and Optimization, 2008, 47(4): 1814–1850.

[19] POLYAKOV A. Nonlinear feedback design for fixed-time stabilization of linear control systems. IEEE Trans. on Automatic Control, 2012, 57(8): 2106–2110.

[20] NING B D, HAN Q L. Prescribed finite-time consensus tracking for multi-agent systems with nonholonomic chained-form dynamics. IEEE Trans. on Automatic Control, 2019, 64(4): 1686–1693.

[21] ZUO Z Y, HAN Q L, NING B D, et al. An overview of recent advances in fixed-time cooperative control of multiagent systems. IEEE Trans. on Industrial Electronics, 2018, 14(6): 2322–2334.

[22] SHI S, GU J, XU S Y, et al. Globally fixed-time high-order sliding mode control for new sliding mode systems subject to mismatched terms and its application. IEEE Trans. on Industrial Electronics, 2019, 67(12): 10776–10786.

[23] SHI S, MIN H F, DING S H. Observer-based adaptive scheme for fixed-time frequency estimation of biased sinusoidal signals. Automatica, 2021, 127: 109559.

[24] BASIN M, SHTESSEL Y, ALDUKALI F. Continuous finite- and fixed-time high-order regulators. Journal of the Franklin Institute, 2016, 353(18): 5001–5012.

[25] TIAN B L, ZUO Z Y, YAN X M, et al. Fixed-time output feedback control scheme for double integrator systems. Automatica, 2017, 80: 17–24.

[26] NI J K, LIU L, LIU C X, et al. Fast fixed-time nonsingular terminal sliding mode control and its application to chaos suppression in power system. IEEE Trans. on Circuits Systems-II: Express Briefs, 2016, 64(2): 151–155.

[27] CRUZ-ZAVALA E, MORENO J, FRIDMAN L. Lyapunov-based design for a class of variable-gain 2nd-sliding controllers with the desired convergence rate. International Journal of Robust and Nonlinear Control, 2018, 28(17): 5279–5296.

[28] SHI S, GU J, XU S Y, et al. Variable-gain second-order sliding mode controller with globally fixed-time stability guarantees. IEEE Trans. on Circuits Systems-II: Express Briefs, 2020, 67(28): 1414–1418.

[29] LOPEZ-RAMIREZ F, POLYAKOV A, EFIMOV D, et al. Finite-time and fixed-time observer design: implicit Lyapunov function approach. Automatica, 2018, 87: 52–60.

[30] MENARD T, MOULAY E, PERRUQUETTI W. Fixed-time

observer with simple gains for uncertain systems. Automatica, 2017, 81: 438–446.
[31] RIOS H, TEEL A. A hybrid fixed-time observer for state estimation of linear systems. Automatica, 2018, 87: 103–112.
[32] BHAT S, BERNSTEIN D. Finite-time stability of continuous autonomous systems. SIAM Journal on Control and Optimization, 2000, 38(3): 751–766.
[33] FILIPPOV A F. Mathematics and its applications. Differential equations with discontinuous right-hand sides. ARSCott F M, ed. Dordrecht: Kluwer Academic Publishers, 1988.
[34] ANGULO M, MORENO J, FRIDMAN L. Robust exact uniformly convergent arbitrary order differentiator. Automatica, 2013, 49(8): 2489–2495.

Biographies

SHI Shang was born in 1990. He received his B. S. and M.S. degrees in control theory from Jiangsu University, Zhenjiang, China, in 2013 and 2015, respectively. He received his Ph.D. degree with the School of Automation, Nanjing University of Science and Technology, Nanjing, China. He is now a lecture in the College of Energy and Electrical Engineering, Hohai University. His research interests include sliding mode control, finite-time control, fixed-time control, and time-delay systems.
E-mail: shishangshang@yahoo.com

ZHANG Guosheng was born in 1997. He received his B.S. degree in automation from Hohai University, Nanjing, China, in 2021. He is currently working toward his M.S. degree with the College of Energy and Electrical Engineering, Hohai University. His research interests include fixed-time control of wheeled mobile robots and sliding mode control.
E-mail: zgs15295770291@163.com

MIN Huifang was born in 1990. She received her M.S. degree from the School of Electrical Engineering and Automation, Jiangsu Normal University, Xuzhou, China, in 2015, and her Ph.D. degree from the School of Automation, Nanjing University of Science and Technology, Nanjing, China, in 2019. She is now a professor in the School of Automation, Nanjing University of Science and Technology, Nanjing. Her research interests include nonlinear adaptive control and stochastic nonlinear control.
E-mail: jiejie1043640772@126.com

HU Yinlong was born in 1987. He is now an associate professor in the College of Energy and Electrical Engineering, Hohai University. He received his B.S. degree in electrical engineering and automation in 2010, and his Ph.D. degree in control theory in 2016, from the School of Automation, Nanjing University of Science and Technology, Nanjing, China. His research interests include passive and semi-active vibration control, nonlinear intelligent control theory and its applications in mechanical and electrical systems.
E-mail: yinlonghu@outlook.com

SUN Yonghui was born in 1980. He received his Ph.D. degree from City University of Hong Kong, Hong Kong, in 2010. He is currently a professor with the College of Energy and Electrical Engineering, Hohai University, Nanjing, China. He has authored more than 80 papers in refereed international journals. His research interests include stability analysis and control of power systems, optimal planning and operation of integrated energy system, optimization algorithms, and data analysis.
E-mail: sunyonghui168@163.com